UNIVERSITY OF LEEDS

This is a repository copy of *Tribochemistry evolution of DDP tribofilms over time using in-situ synchrotron XAS*.

White Rose Research Online URL for this paper:
https://eprints.whiterose.ac.uk/176136/

Version: Accepted Version

Article:
Dorgham, A, Parsaeian, P orcid.org/0000-0001-8393-3540, Azam, A orcid.org/0000-0002-3510-1333 et al. (5 more authors) (2021) Tribochemistry evolution of DDP tribofilms over time using in-situ synchrotron XAS. Tribology International, 160. 107026. ISSN 0301-679X

https://doi.org/10.1016/j.triboint.2021.107026

© 2021, Elsevier. This manuscript version is made available under the CC-BY-NC-ND 4.0 license http://creativecommons.org/licenses/by-nc-nd/4.0/.

Reuse
This article is distributed under the terms of the Creative Commons Attribution-NonCommercial-NoDerivs (CC BY-NC-ND) licence. This licence only allows you to download this work and share it with others as long as you credit the authors, but you can't change the article in any way or use it commercially. More information and the full terms of the licence here: https://creativecommons.org/licenses/

Takedown
If you consider content in White Rose Research Online to be in breach of UK law, please notify us by emailing eprints@whiterose.ac.uk including the URL of the record and the reason for the withdrawal request.

White Rose university consortium
Universities of Leeds, Sheffield & York

eprints@whiterose.ac.uk
https://eprints.whiterose.ac.uk/

Tribochemistry evolution of DDP tribofilms over time using in-situ synchrotron XAS

Abdel Dorgham[†,*], Pourya Parsaeian[†], Abdullah Azam[†], Chun Wang[†], Ardian Morina[†], and Anne Neville[†]

[†]Institute of Functional Surfaces, School of Mechanical Engineering, University of Leeds, Leeds LS2 9JT, UK
[*]Corresponding author: a.dorgham@leeds.ac.uk

ABSTRACT

Ashless dialkyldithiophosphate (DDP) antiwear additives are good candidates to replace the widely used metallic DDPs such as zinc dialkyldithiophosphate (ZDDP), which are less environmentally friendly. A newly designed in-situ tribological rig was utilised to perform in-situ synchrotron X-ray absorption spectroscopy (XAS) in order to examine the decomposition reactions of two types of DDPs; acidic and neutral. The tribological experiments showed that the two DDP additives decomposed to form protective tribofilms on the steel surface, which provided better antiwear protection than ZDDP regardless of the tribofilm thickness. The neutral DDP formed a thinner tribofilm (about 33 nm) than ZDDP (about 41 nm), whereas the tribofilm of the acidic DDP had a much lower thickness (<7 nm) but more superior antiwear protection. The two DDPs also provided lower friction coefficient (<0.1) than the 0.12 provided by ZDDP. The XAS experiments suggest that the DDPs decompose to form initially iron sulphate, which is quickly reduced to sulphide before forming the phosphate layers of the protective tribofilm. These layers consisted initially of iron phosphate of short chains but as rubbing continued organic phosphate with long chains started to form.

Keywords: *ZDDP, DDP, antiwear tribofilm, in-situ tribochemistry, synchrotron XAS*

1 Introduction

Zinc dialkyldithiophosphate (ZDDP) is used extensively in lubricating oils to protect contacting surfaces rubbing against each other by forming on them thin layers of a protective tribofilm [1–3]. However, this additive decomposes to form zinc, sulphur and phosphorus-based products, mainly in the form of zinc (thio)phosphate [4, 5], which pose an environmental hazard especially to catalytic converters leading to increased harmful emissions [6]. Therefore, ZDDP and its decomposition products must be reduced or eliminated completely from lubricating oils to comply with the current and projected oil environmental regulations [7].

Thus far, extensive studies were performed in order to find a proper replacement to ZDDP with a similar antiwear performance [1, 2]. One of the steps taken was to reduce or eliminate zinc, sulphur and phosphorus one-by-one while aiming at maintaining the same functionality. The simplest element to eliminate was zinc in order to obtain ashless dialkyldithiophosphate (DDP) [8–12]. Similar to ZDDP, the DDP additive can be in a neutral or acidic form [13]. The type and number of carbon within these forms can define new subdivisions such as primary or secondary [14]. These types can have different thermal stability [15] starting from aryl with the highest then primary alkyl and finally secondary alkyl, which has the lowest thermal stability. As the decomposition of these additives to form protective tribofilms is a thermally and mechanically-assisted process [16–18], the additive with the lowest thermal stability will typically provide the best wear protection [2]. In addition, Dorgham et al. [19] showed that the antiwear performance of ZDDP additives can have rheological origins, which allow the pads of the formed tribofilms to be squeezed and flow in contact. In terms of friction performance, Zhang et al. [20] recently reported that the boundary friction of primary ZDDP depends on the type of the alkyl chains, i.e. linear chains give lower friction than branched chains. On the other hand, the boundary friction of the secondary ZDDPs was found to be less sensitive to the alkyl structure.

The DDP additive shows very similar characteristics to the ZDDP. For instance, when decomposed under rubbing

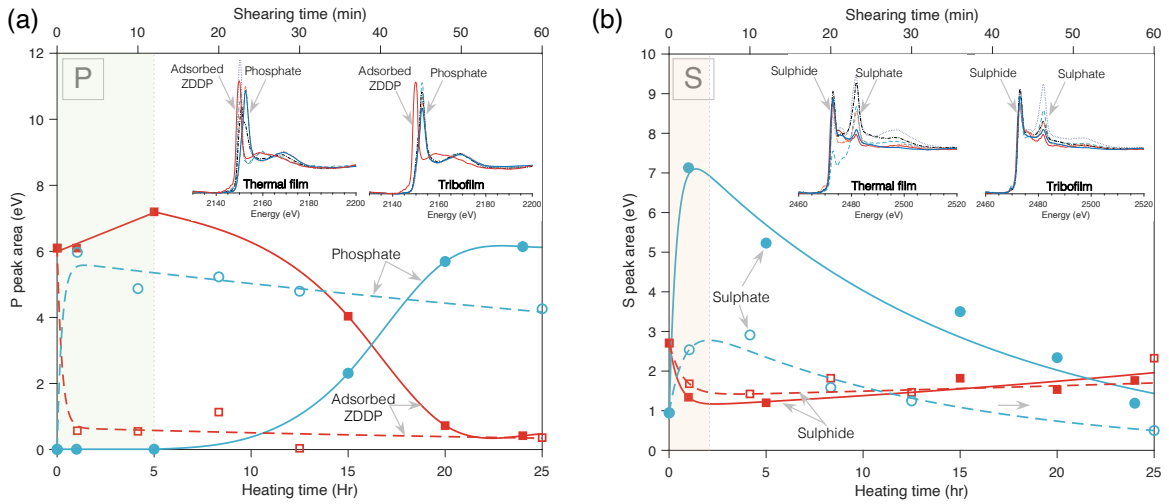

Figure 1. XAS P and S *k*-edges of ZDDP thermal films formed at 80 ^{o}C and tribofilms formed at 2.2 GPa and 80 ^{o}C. a) Evolution of the normalised areas of unreacted/adsorbed ZDDP and phosphate peaks after different heating or rubbing times. b) Evolution of the normalised areas of sulphide and sulphate peaks. The insets of the figures show the evolution of the XAS spectra of the thermal and tribofilms. Adapted from Dorgham et al. [5].

and high temperature, the DDP additive, similar to ZDDP, generate thin layers of a protective tribofilm covering the contact region. However, there is no consensus on whether the DDP additive exhibits a superior [8, 9], similar [10] or inferior [11, 12] wear protection compared to ZDDP. This disparity of the reported antiwear performance might be related to not only the tribofilm composition but also its adhesion, hardness and elasticity.

Several previous studies [11, 13, 21–23] suggested that the tribofilm of the DDP additive is formed predominantly of iron polyphosphate with typically short chains, along with a small amount of sulphur compounds [21, 24, 25]. On the other hand, the ZDDP tribofilm typically consists of zinc (thio)phosphate of variable chain lengths, i.e. the shortest are near the metal surface while the longest are in the outer layers, along with a small content of sulphur species [4, 5, 26]. However, there is no agreement in the literature on the exact temporal changes of the sulphur-based decomposition products exist in both the tribofilms and thermal films, in terms of amount or specificity. Dorgham et al. [4] showed that the ratio of P/O/S of the formed ZDDP tribofilm changes largely in the beginning of the test, but stays constant after the running-in period. In contrast, Zhang et al. [12] reported that the S/P ratio in the case of ZDDP tribofilm does not change throughout the test, whereas in the case of DDP the ratio was found to decrease gradually although the tribofilm thickness was increasing. Roache et al. [27] reported that the higher the phosphorus concentration, along with lower sulfur concentration, the better the antiwear performance of ZDDP tribofilms.

In terms of the specificity of the sulphur species, Dorgham et al. [5, 26] suggested that before the formation of the phosphate-based ZDDP tribo- or thermal film, the ZDDP additive initially decomposes to form metal sulphate, which over heating or rubbing is reduced into predominantly sulphide, as shown in Fig. 1. Hsu [28] also showed that a sulfur-rich base layer exists between the oxide layer on the metal surface and the ZDDP tribofilm. Dörr et al. [29] suggested that sulphide species are dominantly formed from fresh oils but sulfate species increase in concentration when degraded oils are used. Similarily, Kim et al. [13] observed that after long heating time (4 hrs), for the tested neutral DDP, all sulphur appears in the oxidised sulphate, whereas for the tested acidic DDP and ZDDP both sulphides and sulphates were observed. Najman et al. [25] proposed that the metal oxides covering the contacting surfaces can react rapidly with sulphur to form iron sulphate. Such a mechanism was suggested to be part of the decomposition of neutral and acidic DDP additives [30]. On the other hand, Zhang et al. [21] found that the sulphur species in the DDP tribofilm are mainly iron sulphide, whereas in the case of ZDDP iron sulphide is formed initially on the metal surface followed by zinc sulphide.

The wide disparity in the available literature regarding the amount and specificity of the formed sulphur species within the ZDDP and DDP tribofilms can be related to the additive type and the different operating conditions under

Table 1. Summary of the different additives tested in this study.

Coded name	Chemical name	Chemical structure
ZDDP	Zinc dialkyldithiophosphate	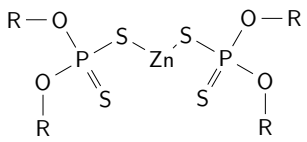
DDP-1	Neutral ashless dialkyldithiophosphate	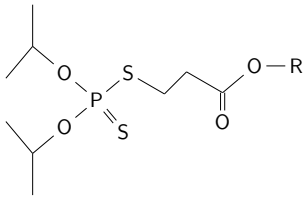
DDP-2	Acidic ashless dialkyldithiophosphate	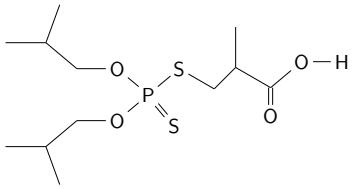

which the tribo- and thermal films were formed. For instance, few previous studies [11, 24] showed that when the operating conditions are harsh, e.g. sliding at high contact pressure in the boundary lubrication regime, the DDP additive decomposes to form iron sulphate near the steel surface. However, under mild operating conditions, e.g. sliding at low contact pressure, the DDP additive decomposes initially to form iron sulphate and sulphides such as FeS and FeS_2. These sulphides can react with the oxide layer on the metal surface over rubbing time to form sulphates. Similarly, Kim et al. [13] reported that when heating the DDP at 170 ^{o}C, its thermal film contains higher sulphate concentration accompanied by a decrease in the sulphide concentration over heating time.

Apart from the additive type and different operating conditions, the conflicting results can be related to the way the data were collected. The majority the previous surface analysis studies were performed ex-situ long after performing the tribological test and typically after rinsing the testing samples with a solvent. This can remove part of the tribofilm and possibly introduce adventitious entities onto the tribofilm. To avoid these possible drawbacks, this study aims at using a newly developed miniature tribological rig coupled with synchrotron XAS [5, 26] in order to examine the composition of DDP tribofilms in-situ as they form. This would enable the continuous monitoring of the decomposition reactions of DDP additives without interfering with the sample initial state.

2 Experimental methods

2.1 Lubricants

The main lubricant used as base oil was a poly-α-olefin (PAO) (4 cSt viscosity at 100 ^{o}C and 0.85 g/cm^3 density). Three different additives were tested as shown in Table 1, which include secondary ZDDP and two types of DDP antiwear additives, i.e. neutral (DDP-1) and acidic (DDP-2). The oil and additives were supplied by Afton Chemicals (UK) and were used as received. All the additives were mixed in the oil such that the P-concentration of 800 ppm is equal across them. In the case of ZDDP, a 0.08% of P corresponds to approximately 0.8 wt.% of ZDDP as the ZDDP is about 10% wt. phosphorus. In the case of DDP-1 and DDP-2 this would correspond to roughly 1.6 wt.% because approximately two DDP molecules with one P atom are equivalent in size to one ZDDP molecule with two P atoms. As the P concentration is the one of paramount importance in forming the P-based tribofilms (of zinc/iron

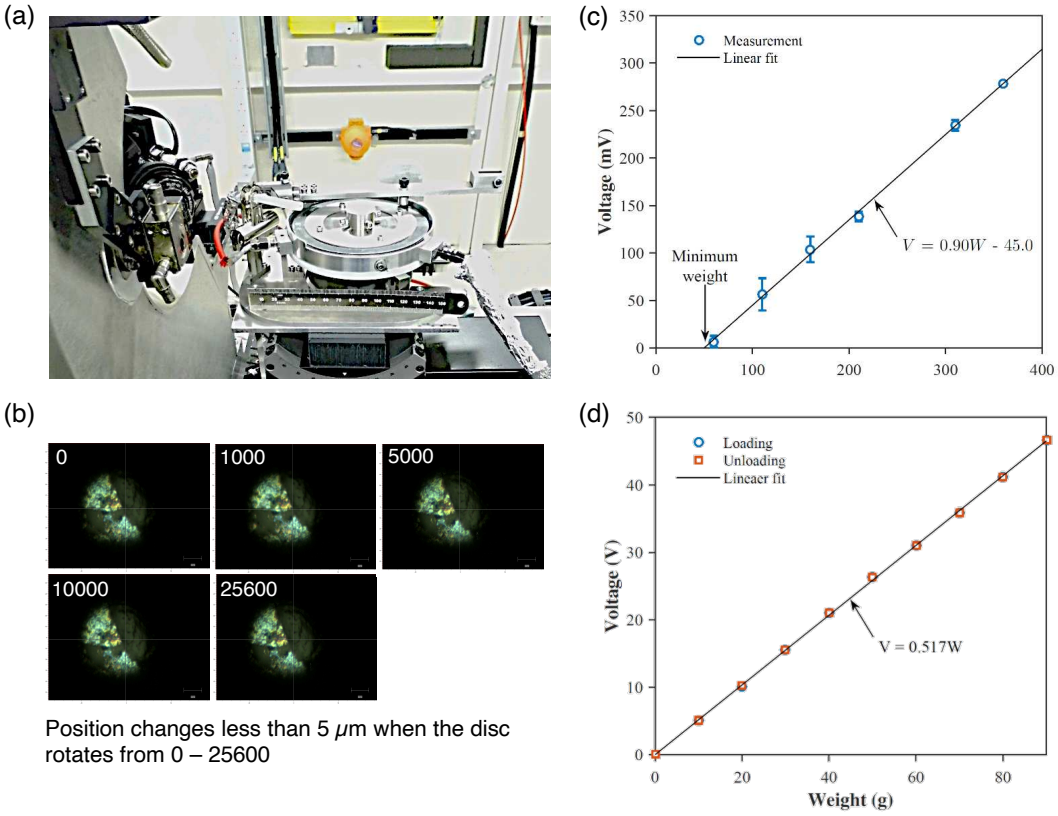

Figure 2. The miniature rig used during the in-situ XAS. (a) the rig in the I18 beamline, (b) position control calibration showing the changes in the position when the motor rotates over 25600 revolutions, (c) and (d) calibration curve of the large and small load compression cell, respectively.

phosphate), keeping this value constant across the different additives would provide a better comparison of the additive capability in forming the phosphate layers than keeping the additives concentrations constant.

2.2 Standard samples

Different standard sulphur and phosphorus samples were used to identify the peaks within the XAS spectra. The sulphur samples comprised S, FeS, FeS_2 from Alfa Aesar and ZnS, $FeSO_4$ and $ZnSO_4$ from Sigma-Aldrich. All these samples were used as received and they had a purity > 99.8%, except FeS_2 which is a natural mineral so its purity was not reported. The phosphorus-based samples were glasses of short chains iron orthophosphate, long chains zinc metaphosphate and mixed zinc-iron polyphosphate of intermediate chains. All glasses were synthesised following Crobu et al. [31].

2.3 Pin-on-disc tribometer

The tribotests were performed using a miniature pin-on-disc tribometer, which is shown in Fig. 2a along with the calibrations of its motor positioning controller (Fig. 2b), large compression load cell (Fig. 2c) and low load cell (Fig. 2d). More details about the rig can be found elsewhere [5, 26]. The pin was a bearing ball (AISI 52100) of 5.5 mm diameter. The disc (AISI 1074) had a thickness of 1 mm. The ball and disc had a hardness of 100 and 64 on Rockwell scale, respectively.

The in-situ tribological experiments were performed at 80 ^{o}C using 50 rpm rubbing speed. The maximum Hertzian contact pressure was 1.0 GPa for all the tribological tests.

2.4 Mini-Traction Machine

Another set of tribological tests were performed ex-situ using the mini-traction machine (MTM) coupled with the spacer-layer imaging method (SLIM) capable of quantifying the tribofilm thickness down to few nanometers. In this setup, a ball (AISI 52100) of 19.05 mm diameter was rubbing against a disc (AISI 52100) of 46 mm diameter. The entrainment speed was 35 mm/s, the slide-to-roll ratio was 5 %, the temperature was 80 ^{o}C and the normal load was 60 N (contact pressure: 1.2 GPa). The purpose of the ex-situ experiments was to follow of the thickness of the tribofilm as it grows/decay over rubbing time, i.e. to answer the questions: a) whether a tribofilm was formed or not and b) if a tribofilm was formed, how did its thickness evolve over time.

2.5 In-situ synchrotron XAS

During the in-situ XAS, the miniature pin-on-disc tribological rig was placed inside a bag filled with inert helium gas in order to reduce the absorbance from air species. The XAS signal was collected after different rubbing times, i.e. 6, 30, 60, 150, 300, 600 and 1200 seconds. Scanning micro-X-ray fluorescence (XRF) images were captured first to identify the wear scar. The XAS signal of P and S k-edges were collected from two locations; one inside and one outside the wear scar. Because of the nature of the XAS experiments, it was extremely difficult to repeat the in-situ tests because of the limited time provided for such experiments in the beamline. The experimental procedures of XRF, XAS, beamline and detector setups were discussed in great detail elsewhere [26]. The spectra were analysed using Athena software (version 0.9.26). The analysis of the XAS data was performed following established procedures outlined by Ravel and Newville [32], which started with the background subtraction followed by the normalisation of the data to remove any dependency on the samples or detector details.

2.6 White light interferometry

The wear scar depth and width were quantified using NPLEX white light interferometer (Bruker, USA). The wear measurements were all based on the disc countersurface. The measurement procedure started with rinsing the disc in heptane. This is followed by removing a small region of the tribofilm using a solution of EthyleneDiamineTetraAcetic acid (EDTA) in distilled water with a concentration of 0.05 M. A droplet from this solution was placed on the wear scar for 60 s [33, 34]. Afterwards, the interference images were collected using a camera and analysed using Vision64 software (Bruker, USA).

3 Results

3.1 Tribofilm thickness

The MTM-SLIM results of the evolution of the tribofilm thickness of ZDDP, DDP-1 and DDP-2 during the ex-situ tribological tests are shown in Fig. 3. The results show that within the first 20 minutes of rubbing, the ZDDP additive formed a tribofilm of similar thickness to the one of DDP-1, i.e. about 13 nm, but still much larger than the one of DDP-2 that had an average thickness of 4 nm. As rubbing continued, the ZDDP additive formed the thickest tribofilm with an average thickness of 63 nm after 40 minutes, which was partly removed to about 41 nm after 60 minutes. On the other hand, the tribofilm of DDP-1 additive continued to grow steadily to about 33 nm after 60 minutes of rubbing. The DDP-2 additive, however, appeared to maintain its ultrathin tribofilm throughout the test, i.e. it had a maximum tribofilm thickness of about 7 nm after 60 minutes of rubbing. It should be noted though that the film thickness measurements represent the first 20 minutes of rubbing only. This means that beyond 20 minutes, the DDPs might end up forming thicker tribofilms in the later stages of the tribological tests.

3.2 Friction and wear

The evolutions of the friction coefficients of the two tested DDP additives are shown in Fig. 4 along with the one of ZDDP antiwear additive as a reference. The ZDDP additive started with a low friction coefficient of about 0.101, which increased gradually to about 0.118, which is the average value of the last five minutes of sliding. This behaviour could be attributed to the progressive formation of a thick and rough ZDDP tribofilm, which can affect the fluid entrainment as suggested originally by Taylor et al. [35] and confirmed recently by Dawczyk et al. [36]. The DDP-1 additive showed a slightly different friction behaviour. Throughout the test, the DDP-1 friction coefficient

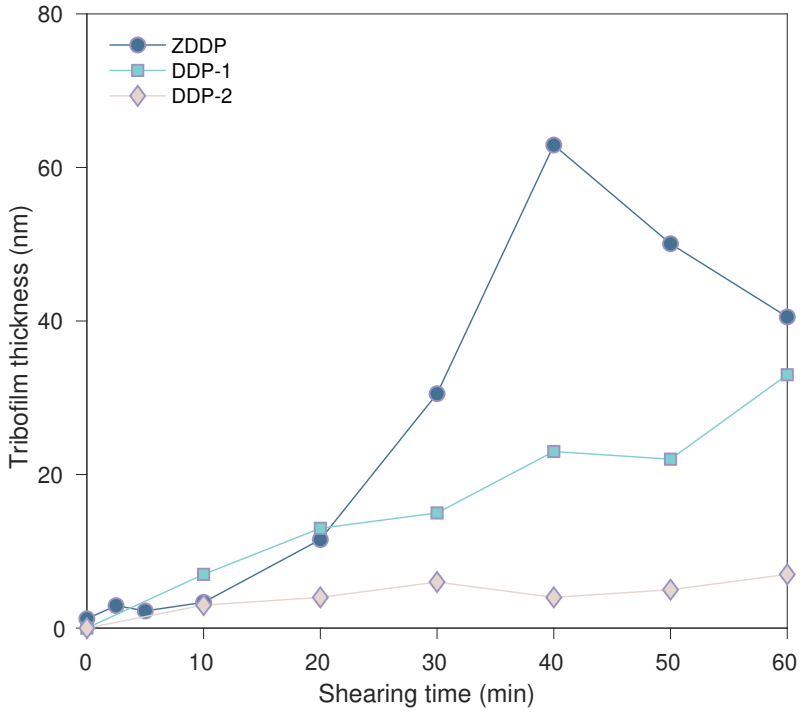

Figure 3. Evolution of the film thickness of ZDDP, DDP-1 and DDP-2 tribofilms over rubbing times during the in-situ tribological experiments.

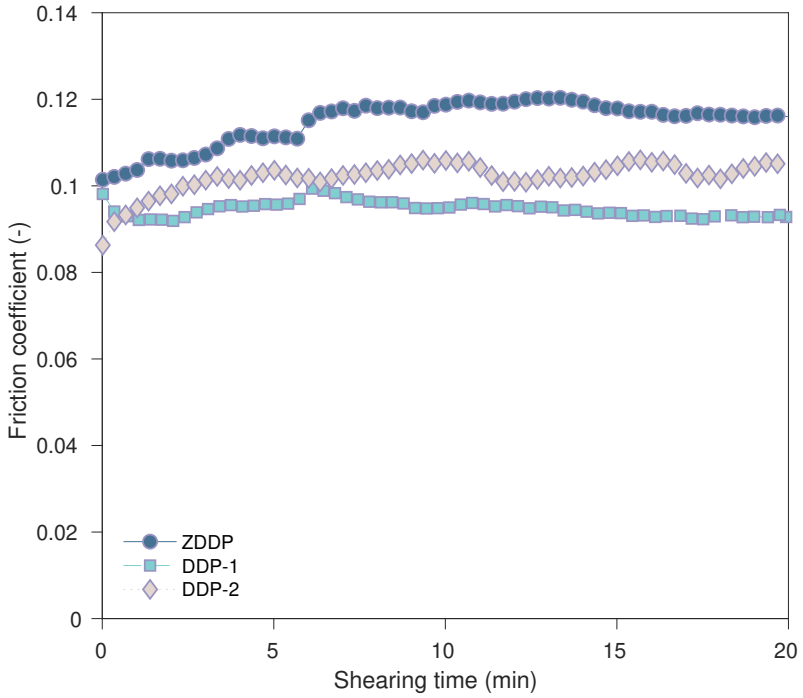

Figure 4. Evolution of the friction coefficient of ZDDP, DDP-1 and DDP-2 tribofilms over rubbing times during the in-situ tribological experiments.

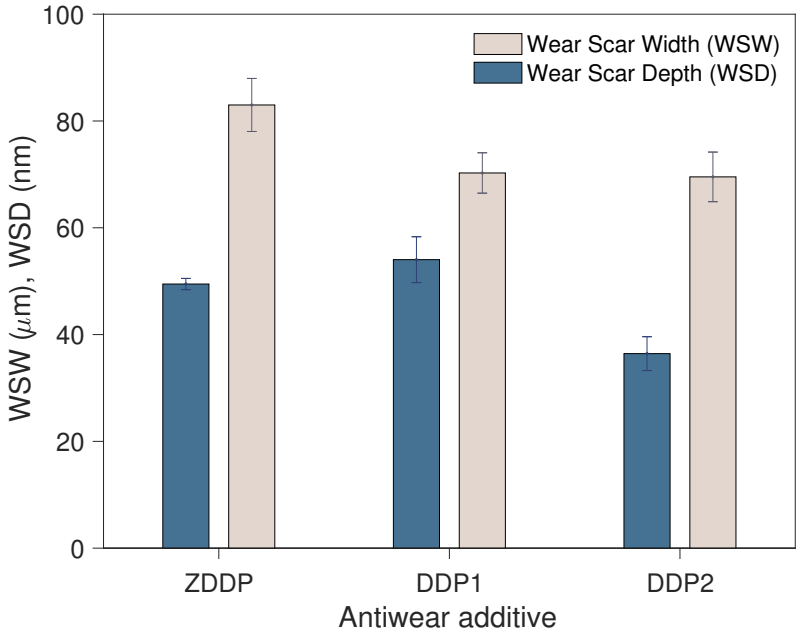

Figure 5. Wear scar width and depth of the XAS discs after the in-situ tribological experiments of ZDDP, DDP-1 and DDP-2 additives.

was low and stable about 0.093. The minor changes occurring from the beginning to the end of the test, compared to the bigger changes in the case of ZDDP, could indicate that the additive decomposed to form a smoother and thinner protective tribofilm.

The friction coefficient of the DDP-2 additive was around 0.104, which is slightly higher than DDP-1 but still lower than ZDDP. It also showed bigger fluctuations than DDP-1 over rubbing time. The origin of this instability can be related to three possible reasons. First, extensive wear and surface damage might have occurred to the steel substrate without the formation of a thick protective antiwear tribofilm. The MTM-SLIM results confirmed that the formed DDP-2 tribofilm is thin. Second, a protective tribofilm is formed, which apart from being thin could have a large roughness, low tenacity or possibly frequent formation and removal cycles. Third, the formed tribofilm consists of long phosphate chains, which means that they can interpenetrate while the two contacting surfaces rub against each other and subsequently increase friction before undergoing depolymerisation and so forth.

The widths and depths of the wear scars for the cases of ZDDP and the two DDP additives are shown in Fig. 5. The results show that, under the same operating conditions, the ashless DDPs axhibited a comparable or superior antiwear performance to that of ZDDP, though the DDP-2 showed the best wear performance. This suggests that, similar to the ZDDP antiwear additive, the ashless DDPs were decomposed to form antiwear tribofilms. However, as the MTM-SLIM showed that the formed DDP-1 and DDP-2 tribofilms are thin, their wear protection appears to originate not only from the formation of a mechanical barrier but also the exact tribochemistry of the tribofilms.

3.3 XAS analysis of standard samples

Fig. 6 shows the synchrotron XAS spectra of different phosphorus and sulphur standard samples, which will be used as references for identifying the different species within the ZDDP and DDP tribofilms. The spectra show that the type of the cation within the phosphate glass can be identified using either the presence of a pre-edge peak (Fe-P) around 2148.0±0.2 eV, or the position of the main phosphate peak (O-P) at 2153.0±0.5 eV. In the glass without iron cations, no pre-edge peak appeared. In addition, as the iron concentration becomes higher in the pure iron phosphate compared to the mixed zinc and iron phosphate, the pre-edge peak becomes higher. Furthermore, the presence of iron cations makes the main phosphate edge peak to appear wider compared to the ones without iron. Moreover, the phosphate edge peak appears to move to a higher energy as the phosphate cation changes from zinc to mixed

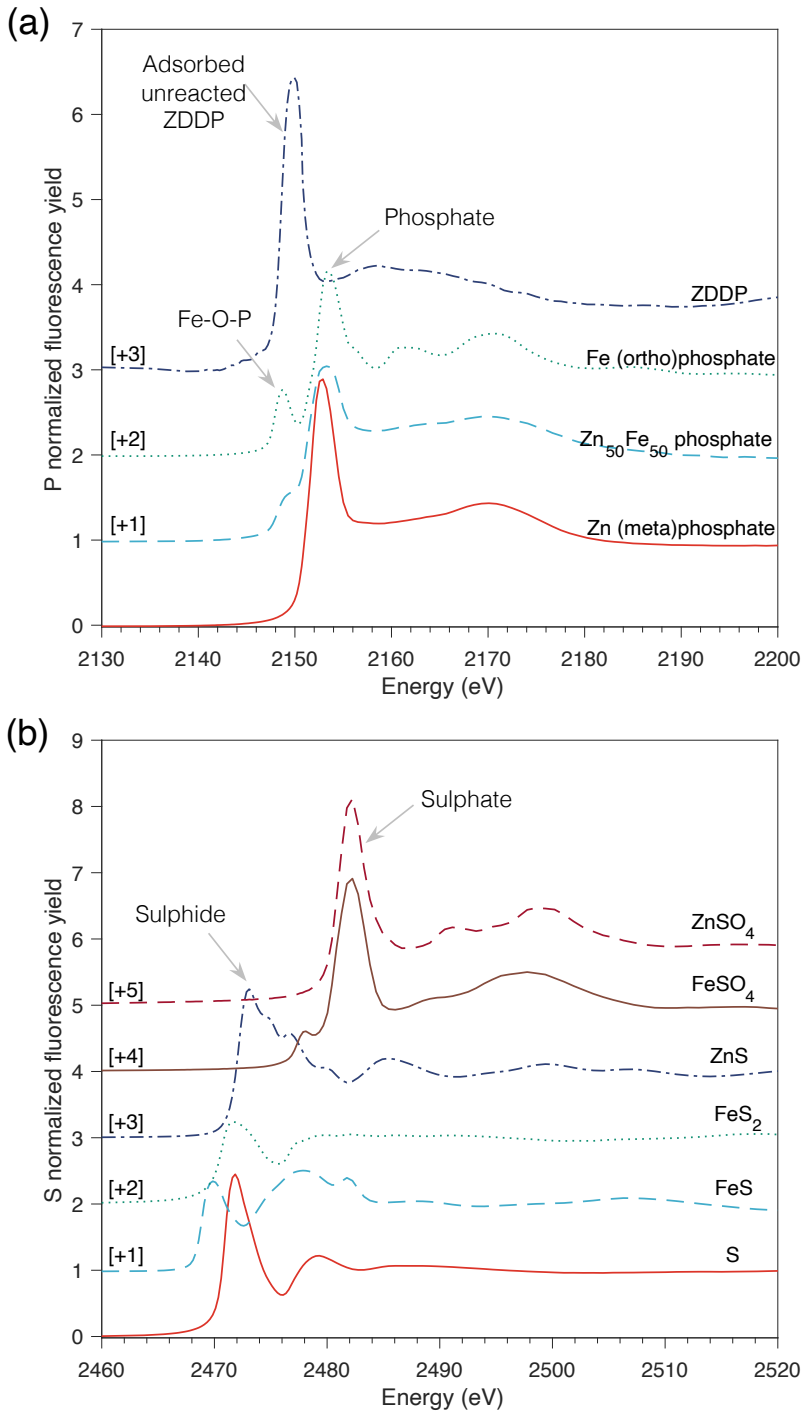

Figure 6. Normalised (a) P and (b) S *k*-edge spectra of different standard compounds.

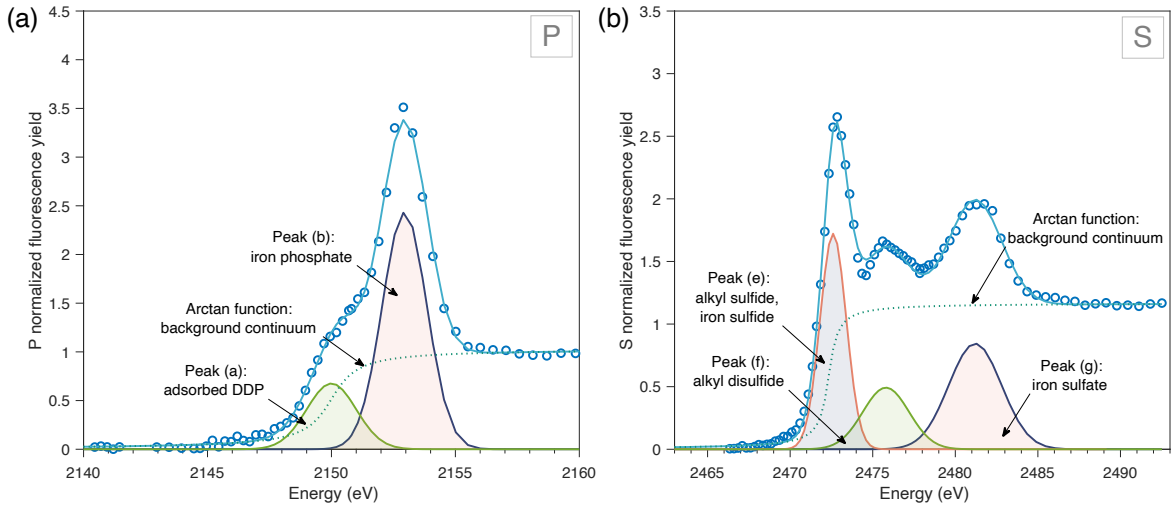

Figure 7. Peak fitting model of the peaks of a) P *k*-edge and b) S *k*-edge of DDP-1 tribofilm formed after 10 minutes of rubbing at 1.0 GPa and 80 ^{o}C.

zinc/iron to iron. The evolution of these different peaks composing the P k-edge will be quantified using the fitting model shown in Fig. 7a by following peak (a) of the unreacted/adsorbed and peak (b) of decomposed phosphate from within the tribofilm layers.

The XAS spectra of the sulphur k-edge of different standard samples are shown in Fig. 6b, which will be used as references to identify the sulphur species within the tribofilms. The results showed that each spectrum is unique in terms of its peaks and their numbers, positions, shapes and heights. In most of the cases, the main edge peak for the different samples can be used alone as a fingerprint. For example, the edge peak of the FeS appeared at 2470.0 eV [11], whereas FeS_2 appeared at 2472.0 eV [25], ZnS appeared at 2473.0 eV [37], and $FeSO_4$ and $ZnSO_4$ both appeared at 2482.0 eV [38, 39]. The latter two samples can be distinguished by observing that in the case of $FeSO_4$ a pre-edge peak is present at 2480.0 eV. The evolution of these peaks composing the S k-edge will be followed using the fitting model shown in Fig. 7b by focusing on the sulphide peaks (e) and (f) and sulphate peak (g).

3.4 XAS analysis of DDP-1 tribofilms

3.4.1 P k-edge spectra

The temporal changes of the P *k*-edge spectra are shown in Fig. 8a. Similar to the ZDDP thermal films [26] and tribofilms reported before [5], which are also shown in Fig. 1, the DDP tribofilm spectra have three distinctive peaks a, b and c. Peak (a) position was around 2150.2 eV, which corresponds to unreacted DDP (P-S or P-R) adsorbed to the steel surface. This is evident from its distinctive appearance before rubbing started. The second peak (b) started to appear at 2152.8 eV only after rubbing commenced. This peak can be assigned to long or short phosphate (P-O) chains, i.e. either containing iron or zinc [38, 40, 41]. Post-edge peak (c) was observed at 2171.0 eV, which gives information regarding the oxidation state of the phosphate [42]. A pre-edge peak (a') at 2148.0 eV, which is a fingerprint of iron, cannot be confirmed for this dataset due to the convoluted noise in the spectra.

The changes in the areas of the unreacted DDP and phosphate peaks at the P *k*-edge can be quantified by fitting these peaks using the fitting model shown in Fig. 7a. The evolution of the areas of the fitted peaks is shown in Fig. 8b after different tribological test times. The first thing to notice is that the DDP tribofilm does not have induction period characterised by the adsorption of the unreacted DDP, i.e. the area of peak (a) increases, without the formation of phosphate layers, i.e. the absence of phosphate peak (b), over a certain period of rubbing time. This behaviour appears to be similar to that of ZDDP tribofilms generated at high contact pressure or the thermal films generated at high temperature [5]. The second thing to notice is that the evolution of the areas of unreacted DDP peak (a) and phosphate peak (b) can be divided into two distinctive phases. The first phase (I) occurred immediately during the first minute of testing. It started directly with the fast decomposition of the unreacted DDP to form metal phosphate.

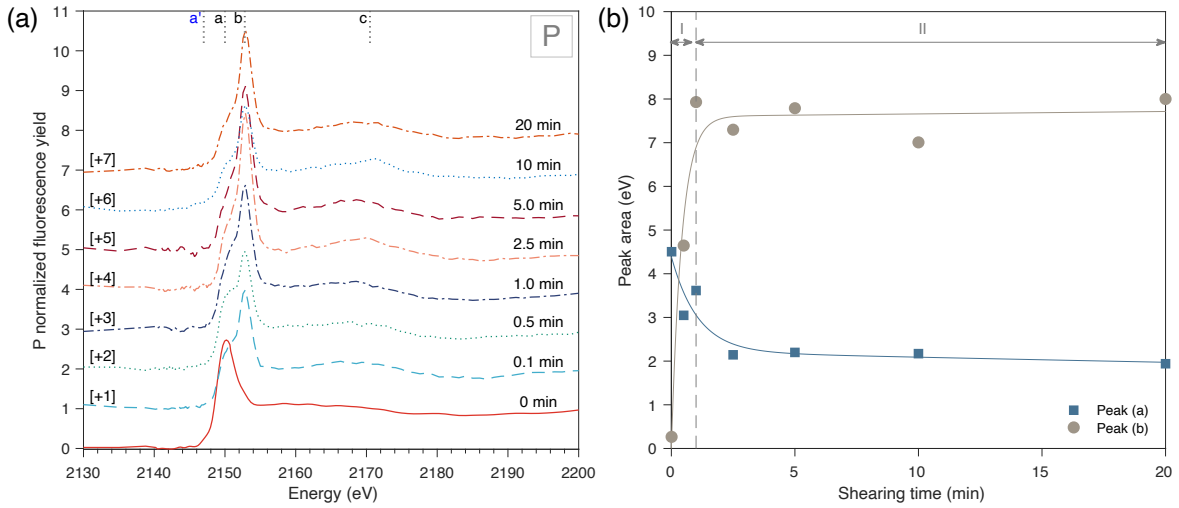

Figure 8. XAS P *k*-edge of DDP-1 tribofilms formed at 1.0 GPa and 80 ^{o}C. a) Evolution of the spectra after different rubbing times, (b) Evolution of the normalised areas of unreacted DDP-1 peak (a) and phosphate peak (b) after different rubbing times.

This is clear by noticing that the peak area of the unreacted DDP decreases at a rate of 0.9 eV/min, whereas the peak area of the phosphate increases at a much faster rate of 7.5 eV/min.

The second phase (II) started after only a few minutes of rubbing. In this phase, minor changes were observed in the peaks areas of the unreacted DDP and phosphate. This might be due to the tribofilm formation and removal that keep the phosphate chains in a balance between polymerisation and depolymerisation thus the tribofilm composition stays relatively constant during the tribological test. This becomes clearer by noticing the difference between the progressively evolving ZDDP tribofilms over rubbing time [5], and the slowly evolving DDP tribofilms, which were reported before [11, 13, 21–23] to generally consist of short chains of iron polyphosphate undergoing minor changes, i.e. polymerisation or depolymerisation over time. This is primarily related to the rapid reaction of the DDP additive, which does not contain any cation, with the substrate covered with iron oxides, which serves as a reservoir for iron cations. The reaction with the iron oxide appears to limit the growth of the short chains of iron phosphate considerably [24].

3.4.2 S k-edge spectra

The temporal chaqnges of the normalised S *k*-edge spectra are shown in Fig. 9a. A pre-edge peak (d') was expected at 2469.5 eV but this peak was absent or possibly very weak, which can suggest the presence of a small concentration of FeS or other iron-based sulphide or sulphate species in the formed tribofilm. Apart from the pre-edge peak, the different spectra showed three distinctive peaks: d, e and f. Peak (d) was observed at 2472.8 eV, which was ascribed to either FeS_2 or alkyl sulphide [37]. Peak (e) appeared at 2476.0 eV, which was ascribed to alkyl disulphide from the adsorbed DDP [38]. Peak (f) appeared at 2481.9 eV, which was attributed to thio (S_4O_4) from the adsorbed DDP, or iron(III) sulphate [38, 39], or possibly iron(III) sulphate.

The temporal changes of the S *k*-edge spectra of the tribofilm inside the wear scar showed a different trend from the one observed in the spectra of the ZDDP tribofilms [5] and thermal films [26]. Initially, during phase (I) after rubbing for a short time, the sulphate concentration decreased, whereas the sulphide concentration increased. With the progression of rubbing, i.e. > 0.1 minutes, the height of the sulphate peak started to increase, whereas the height of the sulphide peaks decreased. Opposite trends were observed after long rubbing times, i.e. > 7.5 minutes.

The qualitative changes in the XAS S *k*-edge spectra can be quantified using the fitting model presented in Fig. 7b to fit the peaks of the sulphides, peaks (d) and (e), and sulphate, peak (f). Fig. 9b shows the temporal changes of the areas of these peaks. During the initial stage of rubbing, i.e. stage (I) in the first minute, the area of sulphate peak (f) appeared to decrease drastically over time with a rate of 1.9 eV/min. However, over the same period, the

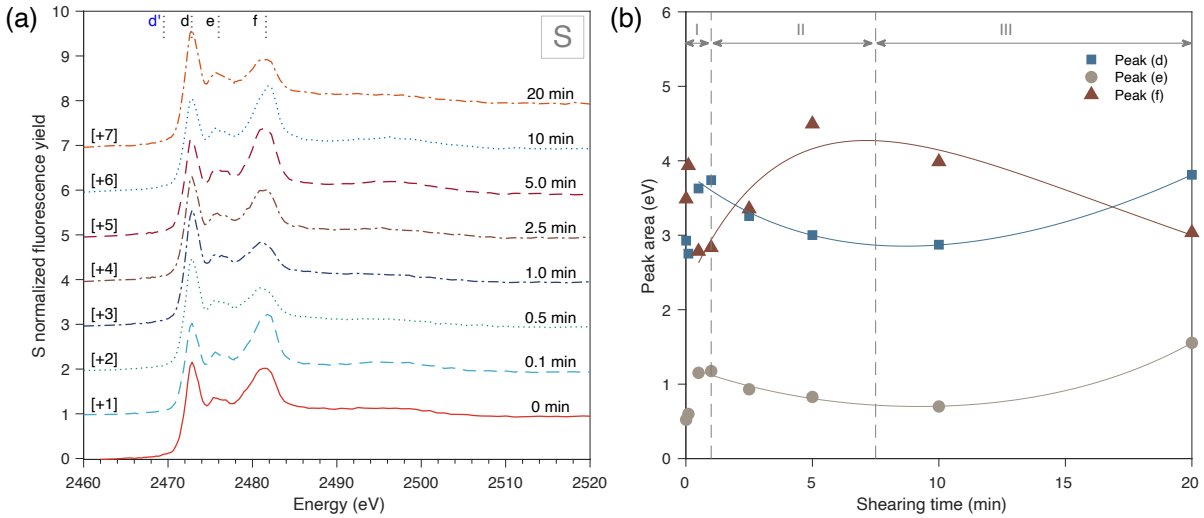

Figure 9. XAS S *k*-edge of DDP-1 tribofilms formed at 1.0 GPa and 80 ^{o}C. a) Evolution of the spectra after different rubbing times, (b) Evolution of the normalised areas of sulphide peaks (d) and (e) and sulphate peak (f) after different rubbing times.

areas of sulphide peak (d) and organic sulphide peak (e) increased with approximately a similar rate of 1.7 eV/min.

With the progression of rubbing, the decomposition of the DDP entered a second phase (II) after the first minute of rubbing, in which the area of the sulphate peak (f) increased gradually over rubbing time with a mean rate of 0.16 eV/min. In contrast, the sulphide peaks (d) and (e) showed an opposite trend of decreasing in area with a rate of 0.16 eV/min and 0.08 eV/min, respectively. The opposite trends can possibly indicate a continuous decomposition of the adsorbed DDP to produce sulphate species. This is in agreement with the results of Kim et al. [13], which examined the decomposition of two different types of DDP additives. One DDP decomposed to form a tribofilm containing only sulphate species, but the other DDP additive decomposed to form sulphides and sulphates. The formation of sulphate species was related to the rapid oxidation reaction of the DDP with the metal oxide layer covering the substrate to form iron sulphate [25]. Neutral and acidic DDPs were reported to have a similar reaction [30].

As rubbing continued, the decomposition of the DDP entered a third phase (III) after the first 7.5 minutes of rubbing. During this phase, a reduction in the peak area of the sulphate peak was observed with a mean rate of 0.1 eV/min. In contrast, an increase in the peak area of the sulphide was observed with a smaller rate of 0.06 eV/min. These trends can be a result of the consumption of the sulphate to form sulphide species.

3.5 XAS analysis of DDP-2 tribofilms

3.5.1 P k-edge spectra

The temporal changes of the P *k*-edge spectra are shown in Fig. 10a. The different spectra show three distinctive peaks: a, b and c. Peak (a), appeared at 2150.0 eV corresponding to unreacted or adsorbed DDP. Peak (b) was observed at 2152.8 eV, which existed after heating but before rubbing commenced. The strong and fast appearance of this peak, which can be ascribed to phosphate, can indicate that the additive has a fast reaction at high temperature that led to its complete decomposition even without the need of rubbing. The formation of phosphate is further confirmed by the fixed position and height of the additional peak (c), which appeared at 2169.5 eV in the high energy post-edge region similar to that appeared in the DDP and ZDDP additives when decomposed to form phosphate. As this post-edge peak can be related to the oxidation state the phosphate [42], its position or height similar to that of phosphate suggests the formation of phosphate species that undergo minor changes from the beginning to the end of the tribotest.

The temporal changes in the areas of peak (a) of the unreacted DDP and peak (b) of the reacted phosphate are shown in Fig. 10b after different rubbing times. The results indicate that in the first minute of the test, i.e. stage (I), the unreacted DDP peak (a) decreased slightly along with a similar slight increase in the reacted phosphate peak (b).

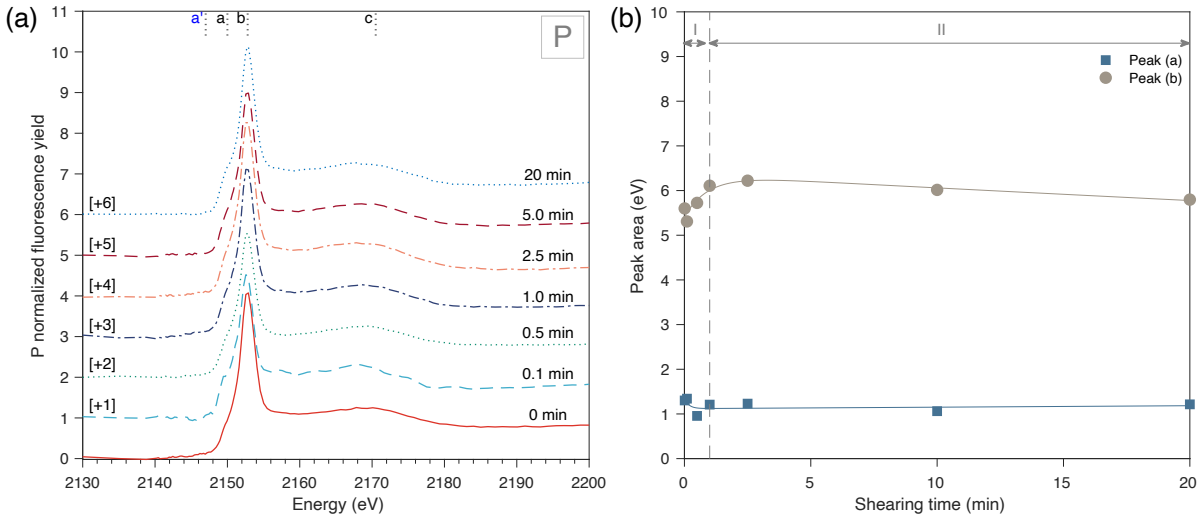

Figure 10. XAS P *k*-edge of DDP-2 tribofilms formed at 1.0 GPa and 80 ^{o}C. a) Evolution of the spectra after different rubbing times, (b) Evolution of the normalised areas of unreacted DDP-1 peak (a) and phosphate peak (b) after different rubbing times.

Following this, throughout stage (II) of the tribotest, rubbing appears to cause a negligible change in the areas of the two peaks. One possible explanation for this trend is the limiting nature of this DDP additive to form a tribofilm under the applied operating conditions. This is confirmed by the ex-situ tests performed using the MTM-SLIM (Fig. 3), which showed that the DDP-2 decomposed to form an ultrathin tribofilm of limited thickness and thus possibly composition as well.

3.5.2 S k-edge spectra

The temporal changes of the normalised spectra of S *k*-edge are shown in Fig. 11a. As discussed before in the case of DDP-1, the spectra of the DDP-2 tribofilms show three distinctive peaks: d, e and f. Peak (d) appeared at 2473.0 eV, which is ascribed to either FeS_2 or alkyl sulphide [37]. Peak (e) appeared at 2476.0 eV corresponding to alkyl disulphide from the adsorbed DDP [38]. Peak (f) was observed at 2481.5 eV, which can be attributed to thio (RS_4) from the adsorbed DDP, or iron(II) sulphate [38, 39], or possibly iron(III) sulphate. A secondary pre-edge peak (d') was also expected at 2469.5 eV. The absence of this peak suggests the absence or low concentration of iron-based sulphide or sulphate species in the tribofilm [38].

The spectra of XAS S *k*-edge can be quantified by fitting the sulphides peaks (d) and (e) and sulphate peak (f) as shown in Fig. 7b. The evolution of these peaks appears to closely resemble that of DDP-1. During the first minute of rubbing, i.e. stage (I), a drastic decrease in the area of the sulphate peak (f) was observed with a rate of 3.3 eV/min. On the other hand, an increase in the areas of the sulphide peak (d) and organic sulphide peak (e) was observed over the same period but with a lower rate of 1.0 eV/min. With the progression of rubbing, the decomposition of the DDP entered a second phase, i.e. stage (II) during which the area of the sulphate peak (f) increased gradually over time with a mean rate of 0.09 eV/min. Similarly, the sulphide peaks (d) and (e) showed a similar trend but their rates of area increase were 0.14 and 0.05 eV/min, respectively. The similar low rates suggest that there is a continuous adsorption of the unreacted DDP on the metal surface. After the first 7.5 minutes of rubbing, the decomposition of the DDP additive entered a third phase, i.e. stage (III), during which the sulphate peak decreased with a mean rate of 0.07 eV/min. In contrast, the sulphide peaks showed a different trend of not changing in area over rubbing time.

These results combined with the observations in the spectra of P *k*-edge suggest that, similar to the case of DDP-1, the DDP-2 additive undergoes a total decomposition to generate a phosphate-based tribofilm. The initial changes in the sulphur are also comparable to the previously reported results [5, 26] for the ZDDP tribo- and thermal films during their induction period, which indicated that initially the additive adsorbs to the steel surface and undergoes reconfiguration affecting the sulphur.

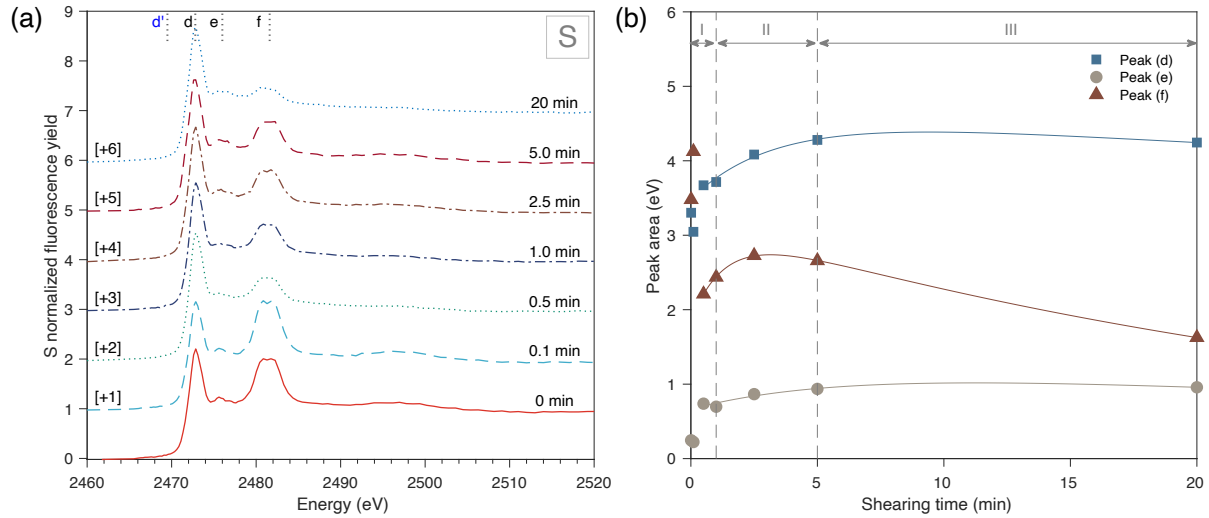

Figure 11. XAS S *k*-edge of DDP-2 tribofilms formed at 1.0 GPa and 80 ^{o}C. a) Evolution of the spectra after different rubbing times, (b) Evolution of the normalised areas of sulphide peaks (d) and (e) and sulphate peak (f) after different rubbing times.

4 Discussion

The DDP additive decomposition process was found in general to be similar to that of ZDDP additive. The XAS results suggest that in the case of DDP-I (Figs. 8 and 9) or DDP-II (Figs. 10 and 11) extensive formation of sulphate species occurs initially. This can be related to the rapid reaction of the DDP the metal oxide on the rubbing surfaces. Such a reaction oxidises sulphur to iron sulphate [25]. A similar mechanism was proposed previously in the cases of neutral and acidic DDPs [30]. As rubbing progresses, a continuous consumption of the sulphate occurs to form more stable sulphide species. The formation of sulphides is in line with the findings of Zhang et al. [21] suggesting that the DDP additive forms mainly FeS. However, several previous studies [13, 25, 30] suggested that it is not in the beginning of the decomposition of DDP additives but rather in the end that sulphate species are formed. This apparent discrepancy is attributed to the wide variations in the testing conditions across the different studies during the tribofilm formation. For instance, some studies [11, 24] reported the presence of iron sulphate in the case of the DDP thermal films and tribofilm generated under high contact pressure. However, under mild contact pressure, in the beginning of rubbing both sulphide and sulphate are present in the generated tribofilm. As rubbing continues, the oxidation of sulphide to sulphate progresses until mainly sulphate can be found in the tribofilm. In comparison, it was reported [5, 26] that in the generated ZDDP tribofilms at high contact pressure, the sulphate/sulphide ratio was much lower than that found in the case of low contact pressure. This was related to the accelerated effect of contact pressure on reducing sulphate into sulphide. It was also reported [5] that at longer rubbing times, the same effect can be achieved, i.e. the sulphate will eventually be reduced into sulphide. Our results also show that the different sulphur species change progressively over time. This suggests that one of the reasons behind the previously reported different sulphur species can be due to the different rubbing times across the tests.

After the formation of the oxide-sulphide mixed layer, a phosphate-based tribofilm starts to form whether in the case of DDP-I or DDP-II additive. The formation of phosphate was evidenced by the considerable rise in the height of peak (b) corresponding to phosphate over the rubbing time, which eventually approached steady state with minor changes. Several previous studies [11, 13, 21–23] suggested that the DDP additives decompose to form mainly short chains of iron-based phosphate. However, a different conclusion can be reached when comparing the temporal changes in the peaks of DDP-1 and DDP-2 along with those from ZDDP, as shown in Fig. 12. Initially, peak (a), which is ascribed to unreacted or adsorbed additive, appears to decrease progressively (Fig. 12a) accompanied by a continuous increase in the phosphate peak (b) (Fig. 12b). As these results are based on the normalised signals, it was suggested [5] that they reflect the evolution of the chain length instead of the tribofilm thickness. Thus, the overall

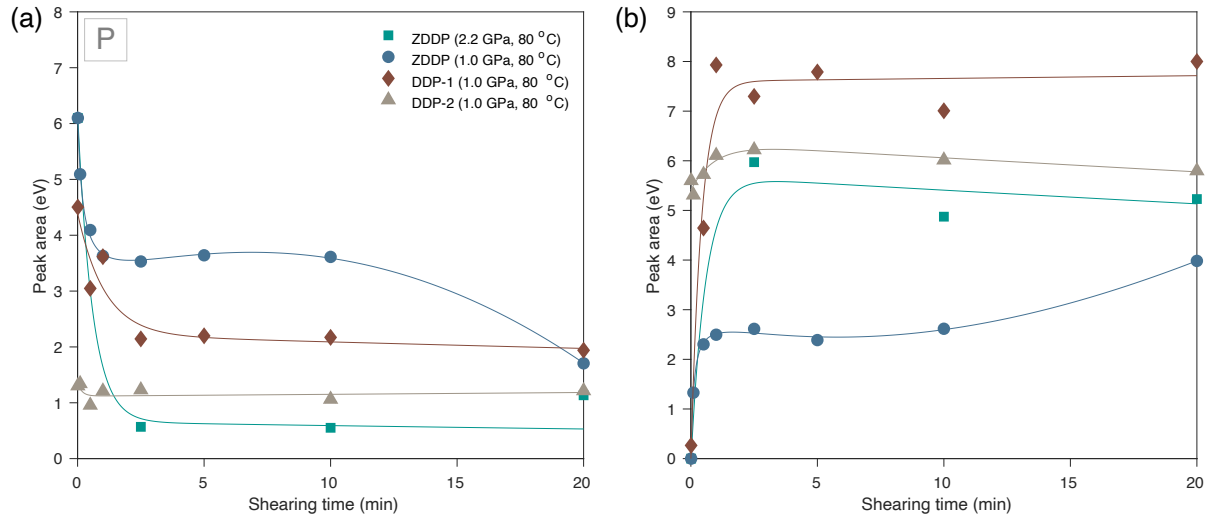

Figure 12. Evolution of the XAS normalised areas of (a) adsorbed ZDDP and DDP peak a, and (b) phosphate peak b after different rubbing times.

results indicate that there is a progressive increase in the chain length of the formed phosphate-based tribofilms of ZDDP or DDP additives until reaching a steady state length. Interestingly, the DDP-1 and DDP-2 additives exhibited the highest chain, even longer than that of ZDDP. However, if the DDP tribofilms contain iron cations, i.e. consists of iron phosphate, the phosphate chains will undergo depolymerisation, which will result ultimately in the formation of short chains [1, 24]. The XAS results could not conclude the presence of iron due to the convoluted noise in the data. However, if iron was present with a high concentration, a clear pre-edge peak would have been observed with a height higher than the noise level, as shown in Fig. 6. The absence of this peak suggests either no iron is present, or it is present but with a low concentration or over patchy areas. We can only speculate that initially iron phosphate might have formed when the decomposed additive has a direct access to the metal surface. However, as more iron phosphate with short chains is formed, the phosphate will not have access to the iron cations. This is the case here because of the relatively mild operating conditions, i.e. sliding at low contact pressure, as evidenced by the small observed wear, i.e. small wear scar width and depth. Thus, in the outer layers no iron phosphate might form but instead organic phosphate with long chains might be present [21, 43]. These long chains appear to be a contributing factor in the observed decrease in the measured friction and wear, as summarised in Table 2. A similar behaviour was reported before for the case of ZDDP [4] that the longer the phosphate chains, the easier their alignment in the direction of shear. The aligned chains will have different beneficial effects on friction and wear. First, they can

Table 2. Summary of the friction, wear and tribochemistry results of the different tested additives.

Property	ZDDP	DDP-1	DDP-2
Friction coefficient (-)	0.118	0.093	0.105
Wear scar depth (μm)	48	52	40
Wear scar width (μm)	79	69	66.4
	Chain length		
Adsorbed ZDDP peak (a)	1.7	1.9	1.2
Phosphate peak (b)	4.0	8.0	5.8
b/a ratio	2.4	4.1	4.9
Sulphate/sulphide f/d ratio	4.0	0.8	0.4

reduce the shear strength between the rubbing surfaces. Second, they can increase the local effective viscosity in the contact zone. Third, they can cover more of the contacting surfaces, which in turn can increase the protection of the rubbing surfaces from direct contact that helps reduce both wear and friction. The observed friction progression might also be linked to the alkyl side chains. For example, Zhang et al. [20] reported that the boundary friction of primary ZDDP depends on the type of the alkyl chains, i.e. linear chains give lower friction than branched chains. On the other hand, the boundary friction of the secondary ZDDPs was less sensitive to the alkyl structure.

5 Conclusion

In the case of the DDP additives rubbed between uncoated bare steel surfaces, the results suggest that the decomposition reaction is similar to that of ZDDP and consists of multiple steps including the formation of several intermediates, as follows:

- Prior to any tribofilm formation, the unreacted DDP adsorbs to the substrate such that the two sulphur atoms of every molecule are near the substrate to achieve maximum coverage.
- Partial decomposition of the adsorbed additive occurs through losing sulphur, which is oxidised at once into sulphates due to its fast reaction with the metal oxides on the substrate.
- As rubbing continues and the running-in period ends, mainly sulphide is formed.
- The adsorbed molecules undergo full decomposition to generate a protective tribofilm consisting of short chain iron phosphate undergoing minor changes over time.
- At mild operating conditions, e.g. sliding at low contact pressure, as more iron phosphate is formed, the phosphate will not have direct access to iron cations from the metal surface, thus organic phosphate with long chains will start to form.

After this, a balance appears to occur between the removal and formation of the tribofilm that keeps the phosphate glass composition and tribofilm thickness relatively constant during the tribotest period.

Acknowledgment

This work is supported by the Engineering and Physical Sciences Research Council (grant number EP/R001766/1) as a part of ‘Friction: The Tribology Enigma’ (www.friction.org.uk), a collaborative Programme Grant between the universities of Leeds and Sheffield.

References

1. A. Dorgham, A. Neville, A. Morina, Tribochemistry and morphology of p-based antiwear films, in: Advanced Analytical Methods in Tribology, Springer, 2018, pp. 159–214.
2. H. Spikes, The History and Mechanisms of ZDDP, Tribology Letters 17 (3) (2004) 469–489.
3. M. A. Nicholls, T. Do, P. R. Norton, M. Kasrai, G. Bancroft, Review of the lubrication of metallic surfaces by zinc dialkyl-dithiophosphates, Tribology International 38 (1) (2005) 15–39.
4. A. Dorgham, A. Azam, A. Morina, A. Neville, On the transient decomposition and reaction kinetics of zinc dialkyldithiophosphate, ACS applied materials & interfaces 10 (51) (2018) 44803–44814.
5. A. Dorgham, P. Parsaeian, A. Neville, K. Ignatyev, F. Mosselmans, M. Masuko, A. Morina, In situ synchrotron xas study of the decomposition kinetics of zddp triboreactive interfaces, RSC advances 8 (59) (2018) 34168–34181.
6. J. Andersson, M. Antonsson, L. Eurenius, E. Olsson, M. Skoglundh, Deactivation of diesel oxidation catalysts: Vehicle-and synthetic aging correlations, Applied Catalysis B: Environmental 72 (1) (2007) 71–81.
7. API, Engine oil licensing and certification system, Tech. Rep. API 1509, American Petroleum Institute (2014).

8. B. Kim, R. Mourhatch, P. B. Aswath, Properties of tribofilms formed with ashless dithiophosphate and zinc dialkyl dithiophosphate under extreme pressure conditions, Wear 268 (3) (2010) 579–591.
9. X. Fu, W. Liu, Q. Xue, The application research on series of ashless p-containing ep and aw additives, Industrial lubrication and tribology 57 (2) (2005) 80–83.
10. R. Sarin, A. Gupta, D. Tuli, A. Verma, M. Rai, A. Bhatnagar, Synthesis and performance evaluation of o, o-dialkylphosphorodithioic disulphides as potential antiwear, extreme-pressure and antioxidant additives, Tribology international 26 (6) (1993) 389–394.
11. M. Najman, M. Kasrai, G. Bancroft, Chemistry of antiwear films from ashless thiophosphate oil additives, Tribology Letters 17 (2) (2004) 217–229.
12. Z. Zhang, E. Yamaguchi, M. Kasrai, G. Bancroft, Tribofilms generated from ZDDP and DDP on steel surfaces: Part 1, growth, wear and morphology, Tribology Letters 19 (3) (2005) 211–220.
13. B. Kim, V. Sharma, P. B. Aswath, Chemical and mechanistic interpretation of thermal films formed by dithiophosphates using xanes, Tribology International 114 (2017) 15–26.
14. Z. Pawlak, Tribochemistry of lubricating oils, Vol. 45, Elsevier, 2003.
15. L. R. Rudnick, Lubricant additives: chemistry and applications, CRC Press, 2009.
16. A. Dorgham, P. Parsaeian, A. Azam, C. Wang, A. Morina, A. Neville, Single-asperity study of the reaction kinetics of p-based triboreactive films, Tribology International 133 (2019) 288–296.
17. N. Gosvami, J. Bares, F. Mangolini, A. Konicek, D. Yablon, R. Carpick, Mechanisms of antiwear tribofilm growth revealed in situ by single-asperity sliding contacts, Science 348 (6230) (2015) 102–106.
18. N. Gosvami, I. Lahouij, J. Ma, R. Carpick, Nanoscale in situ study of zddp tribofilm growth at aluminum-based interfaces using atomic force microscopy, Tribology International 143 (2020) 106075.
19. A. Dorgham, A. Azam, P. Parsaeian, C. Wang, A. Morina, A. Neville, Nanoscale viscosity of triboreactive interfaces, Nano Energy 79 105447.
20. J. Zhang, M. Ueda, S. Campen, H. Spikes, Boundary friction of zddp tribofilms, Tribology Letters 69 (1) (2021) 1–17.
21. Z. Zhang, E. Yamaguchi, M. Kasrai, G. Bancroft, X. Liu, M. Fleet, Tribofilms generated from zddp and ddp on steel surfaces: Part 2, chemistry, Tribology Letters 19 (3) (2005) 221–229.
22. M. Najman, M. Kasrai, G. Bancroft, A. Miller, Study of the chemistry of films generated from phosphate ester additives on 52100 steel using X-ray absorption spectroscopy, Tribology Letters 13 (3) (2002) 209–218.
23. M. Najman, M. Kasrai, G. Bancroft, B. Frazer, G. De Stasio, The correlation of microchemical properties to antiwear (AW) performance in ashless thiophosphate oil additives, Tribology Letters 17 (4) (2004) 811–822.
24. Z. Zhang, M. Najman, M. Kasrai, G. Bancroft, E. Yamaguchi, Study of interaction of ep and aw additives with dispersants using xanes, Tribology Letters 18 (1) (2005) 43–51.
25. M. Najman, M. Kasrai, G. Bancroft, Investigating binary oil additive systems containing p and s using x-ray absorption near-edge structure spectroscopy, Wear 257 (1) (2004) 32–40.
26. A. Dorgham, A. Neville, K. Ignatyev, F. Mosselmans, A. Morina, An in situ synchrotron xas methodology for surface analysis under high temperature, pressure, and shear, Review of Scientific Instruments 88 (1) (2017) 015101.
27. D. C. Roache, C. H. Bumgardner, Y. Zhang, D. Edwards, D. DeGonia, B. Rock, X. Li, Chemo-mechanical characterization of phosphorus and sulfur containing ashless tribofilms on hypoid gear teeth, Tribology International (2021) 106926.
28. C.-J. Hsu, J. Barrirero, R. Merz, A. Stratmann, H. Aboulfadl, G. Jacobs, M. Kopnarski, F. Mücklich, C. Gachot, Revealing the interface nature of zddp tribofilm by x-ray photoelectron spectroscopy and atom probe tomography, Industrial Lubrication and Tribology.
29. N. Dörr, J. Brenner, A. Ristić, B. Ronai, C. Besser, V. Pejaković, M. Frauscher, Correlation between engine oil degradation, tribochemistry, and tribological behavior with focus on zddp deterioration, Tribology Letters 67 (2) (2019) 1–17.
30. M. Najman, M. Kasrai, G. Michael Bancroft, R. Davidson, Combination of ashless antiwear additives with metallic detergents: interactions with neutral and overbased calcium sulfonates, Tribology International 39 (4)

(2006) 342–355.
31. M. Crobu, A. Rossi, F. Mangolini, N. D. Spencer, Chain-length-identification strategy in zinc polyphosphate glasses by means of xps and tof-sims, Analytical and bioanalytical chemistry 403 (5) (2012) 1415–1432.
32. B. Ravel, M. Newville, ATHENA and ARTEMIS: interactive graphical data analysis using IFEFFIT, Physica Scripta 2005 (T115) (2005) 1007.
33. J. Benedet, J. H. Green, G. D. Lamb, H. A. Spikes, Spurious mild wear measurement using white light interference microscopy in the presence of antiwear films, Tribology Transactions 52 (6) (2009) 841–846.
34. K. Topolovec-Miklozic, T. R. Forbus, H. A. Spikes, Film thickness and roughness of zddp antiwear films, Tribology Letters 26 (2) (2007) 161–171.
35. L. Taylor, A. Dratva, H. Spikes, Friction and wear behavior of zinc dialkyldithiophosphate additive, Tribology transactions 43 (3) (2000) 469–479.
36. J. Dawczyk, N. Morgan, J. Russo, H. Spikes, Film thickness and friction of zddp tribofilms, Tribology Letters 67 (2) (2019) 1–15.
37. K. Masenelli-Varlot, M. Kasrai, G. Bancroft, G. De Stasio, B. Gilbert, E. Yamaguchi, P. Ryason, Spatial distribution of the chemical species generated under rubbing from ZDDP and dispersed potassium triborate, Tribology Letters 14 (3) (2003) 157–166.
38. Z. Zhang, M. Kasrai, G. Bancroft, E. Yamaguchi, Study of the interaction of ZDDP and dispersants using X-ray absorption near edge structure spectroscopy – Part 1: Thermal chemical reactions, Tribology Letters 15 (4) (2003) 377–384.
39. M. Najman, M. Kasrai, G. Bancroft, X-ray absorption spectroscopy and atomic force microscopy of films generated from organosulfur extreme-pressure (EP) oil additives, Tribology Letters 14 (4) (2003) 225–235.
40. M. A. Nicholls, T. Do, P. R. Norton, G. M. Bancroft, M. Kasrai, T. W. Capehart, Y.-T. Cheng, T. Perry, Chemical and mechanical properties of zddp antiwear films on steel and thermal spray coatings studied by xanes spectroscopy and nanoindentation techniques, Tribology Letters 15 (3) (2003) 241–248.
41. A. Morina, H. Zhao, J. F. W. Mosselmans, In-situ reflection-xanes study of zddp and modtc lubricant films formed on steel and diamond like carbon (dlc) surfaces, Applied Surface Science 297 (2014) 167–175.
42. E. D. Ingall, J. A. Brandes, J. M. Diaz, M. D. de Jonge, D. Paterson, I. McNulty, W. C. Elliott, P. Northrup, Phosphorus k-edge XANES spectroscopy of mineral standards, Journal of synchrotron radiation 18 (2) (2011) 189–197.
43. A. Gauthier, H. Montes, J. Georges, Boundary lubrication with tricresylphosphate (tcp). importance of corrosive wear, ASLE TRANSACTIONS 25 (4) (1982) 445–455.